Excerpt from the Proceedings of the 2011 COMSOL Conference in Boston

Porous Media Based Model for Deep-Fat Vacuum Frying Potato Chips

Alexander Warning*[1], Ashish Dhall[1], Diana Mitrea[1], & Ashim K. Datta[1]
[1]Department of Biological and Environmental Engineering, Cornell University
*Corresponding author: 175 Riley-Robb Hall Ithaca, NY 14853-5701, adw88@cornell.edu

Abstract:

Vacuum frying is an alternative method to the traditional atmospheric deep-fat frying that offers the health benefits associated with lower concentrations of acrylamide and less adverse effects on oil quality while still preserving the natural color and flavor of the product.

A multiphase porous media model involving heat and mass transfer within a potato chip was implemented in a commercial CFD program. Simulations were run at different frying pressures of 1.33 kPa, 9.89 kPa, 16.7 kPa, and 101 kPa. Good agreement between predicted and literature experimental moisture, oil, and acrylamide content was obtained. Regardless of fryer pressure, the model showed the core pressure reached approximately 40 kPa higher than the surface. The model modified Darcy"s law to account for the Klinkenberg effect. The model demonstrated that acrylamide formation could be modeled as a function of chip temperature rather than the more general oil temperature.

Keywords: Porous media, Klinkenberg effect, Acrylamide

1. Introduction

Vacuum frying offers a solution with advantages over atmospheric frying such as possibly reducing oil content, preserving natural color and flavor, reducing adverse effects on oil quality (Garayo and Moreira, 2002) and lowering acrylamide (AA) formation (Granda, 2005). Several companies in Asia already utilize vacuum frying processes for fruits, vegetables, fish, and shellfish (Moreira, 2010).

Vacuum frying refers to the process of lowering the pressure preferably below 6.65 kPa (Moreira, 2010) within the fryer in order to cook the food with a lower oil temperature. Since frying can almost be thought of as a drying process, its main goal is to remove moisture while creating certain texture and organoleptic properties.

Mathematical modeling of vacuum frying of potato chips deepens the understanding that experimentation could not provide by itself. Experimentation is unable to measure the pressure, moisture, oil, temperature, and acrylamide (a neurotoxin) distributions reliably inside a product this small. One example of modeling"s benefits is in the resolution of the conflict about whether vacuum frying encourages or discourages oil absorption (Da Silva and Moreira, 2008).

2. Model Formulation

2.1 Model Development and Schematic

A multiphase porous media model is developed describing heat, mass, and momentum transfer within a potato chip during vacuum frying following the work of Halder et al. (2007) for atmospheric frying of restructured potato. The pores are filled with three transportable phases: liquid water, oil, or gas (mixture of water vapor and air). Figure 1 shows the schematic. The model considers 1D heat and mass transfer in the *z*-direction since the lateral surface area of a chip only makes up 6.25% of the total area. Mass and energy conservation equations are developed which include diffusive, capillary, and convective transport. Momentum conservation is developed from Darcy"s equation. A non-equilibrium water evaporation rate and a kinetic model for acrylamide formation based on chip temperature are used.

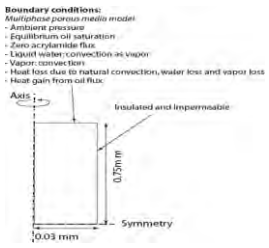

Figure 1. Frying model schematic

2.2 Governing Equations

The governing equations used in this paper are from the original atmospheric frying model (Halder et al., 2007).

2.2.1 Mass Balance Equations

The conservation of mass for water (Eq.1) and oil (Eq. 2) enable the calculation of each species" respective saturation value while acrylamide (Eq. 3) is transported with water and its saturation is negligible.

$$\frac{\partial}{\partial t}(\varphi\rho_w S_w)+\underbrace{\nabla\bullet(u_w\rho_w)}_{\substack{\text{Bulkflow}\\ \text{flux of water}}}=\underbrace{\nabla\bullet\left(D_{w,cap}\nabla(\varphi\rho_w S_w)\right)}_{\text{Diffusive flux of water}}-\dot{I} \quad (1)$$

$$\frac{\partial}{\partial t}(\varphi\rho_o S_o)+\underbrace{\nabla\bullet(u_o\rho_o)}_{\substack{\text{Bulkflow}\\ \text{flux of oil}}}=\underbrace{\nabla\bullet\left(D_{o,cap}\nabla(\varphi\rho_o S_o)\right)}_{\text{Diffusive flux of oil}} \quad (2)$$

$$\frac{\partial}{\partial t}c_{AA}+\nabla\bullet(u_w S_w\varphi c_{AA})=\nabla\bullet\left(D_{AA}\nabla\left(\left\{S_w\varphi+(1-\varphi)\right\}c_{AA}\right)\right)+r_{AA} \quad (3)$$

In the above equations, $\dot{I}=100S_g\varphi\left(\rho_{v,eq}-\rho_v\right)$ is the non-equilibrium evaporation rate of water. Additionally, ρ_i, $D_{i,cap}$, and u_i are density, capillary diffusivity, and velocity of their respective species. The porosity is 0.88. The diffusivities are $D_{w,cap}=1\times10^{-8}e^{-2.8+2M}$, $D_{o,cap}=1.22\times10^{-8}e^{-2.8+2\Omega}$, and $D_{AA} = 4.22\times10^{-15}T/\mu_w$ with dry basis moisture content $M=\varphi S_w\rho_w/(1-\varphi)\rho_s$ and dry basis oil content $\Omega=\varphi S_o\rho_o/(1-\varphi)\rho_s$.

Granda (2005) proposed separate models to explain acrylamide formation for atmospheric frying (Eq. (4)) and vacuum frying (Eq. (5)). In her models, the temperature was based on the oil temperature but not actually on the temperature within the potato. For this simulation, the temperature will be based on the potato and not that of the oil. This slight change increases the understanding of acrylamide formation kinetics especially for potato products thicker than a chip.

$$\frac{d\left(c_{AA}(t)\right)}{dt}=\frac{14.9A\exp\left(\frac{-2625.8}{T}\right)\exp\left\{-14.9\exp\left(\frac{-2625.8}{T}\right)(t-t_o)\right\}}{\left(1+\exp\left\{-14.9\exp\left(\frac{-2625.8}{T}\right)(t-t_o)\right\}\right)^2} \quad (4)$$

$$\frac{d\left(c_{AA}(t)\right)}{dt}=505498C_o\exp\left(\frac{-7344.14}{T}\right)\exp\left[505498\exp\left(\frac{-7344.14}{T}\right)t\right] \quad (5)$$

The pressure difference between the gas pressure and capillary pressure is what causes the flux of liquid water or oil. Capillary pressure is a function of moisture content and temperature.

The gas inside the potato is a mixture of water vapor and air with respective mass fractions ω_v and ω_a. The following mass conservation Eq. (6) is used with binary diffusion, $D_{eff,g}=2.13(T/273)^{1.8}/P$ in place of capillary diffusion.

$$\frac{\partial}{\partial t}\left(\varphi\rho_g S_g\omega_v\right)+\underbrace{\nabla\bullet\left(u_g\rho_g\omega_v\right)}_{\text{Bulk flow flux}}=\underbrace{\nabla\bullet\left(\varphi S_g\frac{C_g^2}{\rho_g}M_a M_v D_{eff,g}\nabla x_v\right)}_{\text{Binary diffusion}}+\dot{I} \quad (6)$$

$$\omega_a+\omega_v=1 \quad (7)$$

Gas saturation is calculated from the requirement that the saturations must equal unity while the pressure is calculated from:

$$\frac{\partial}{\partial t}\left(\varphi\rho_g S_g\right)+\nabla\bullet\left(-\rho_g\frac{k_{in,g}^p k_{r,g}^p}{\mu_g}\nabla P\right)=\dot{I} \quad (8)$$

2.2.2 Momentum Balance Equation

In place of the Navier-Stokes equation, Darcy"s law is used for the momentum conservation equation.

$$u_i=-\frac{k_{in,i}^p k_{r,i}^p}{\mu_i}\nabla P \quad (9)$$

2.2.3 Energy Balance Equation

The energy equation for the potato includes conduction, convection due to movement of water, vapor and air inside the potato, and evaporation.

$$\frac{\partial}{\partial t}\left(\rho_{eff}c_{p,eff}T\right)+\nabla\bullet\left(\left(\rho c_p u\right)_{fluid}T\right)=\nabla\bullet\left(k_{eff}\nabla T\right)-\lambda\dot{I} \quad (10)$$

In Eq. (10), λ is latent heat of evaporation and is a function of pressure, P. The effective properties of the liquid, solid and gas are constantly changing through the frying process as each component"s mass and volume fraction are changing. Below, m_i is the respective mass fractions of each species.

$$\rho_{eff}=(1-\varphi)\rho_s+\varphi\left(S_w\rho_w+S_g\rho_g+S_o\rho_o\right) \quad (11)$$

$$c_{p.eff}=m_g\left(\omega_v c_{p,v}+\omega_a c_{p,a}\right)+m_w c_{p,w}+m_s c_{p,s}+m_o c_{p,o} \quad (12)$$

$$(\rho c_p u)_{fluid} = (\rho_w u_w - D_{w,cap}\nabla(\varphi S_w \rho_w))c_{p,w} + (\rho_o u_o - D_{o,cap}\nabla(\varphi S_o \rho_o))c_{p,o} + \rho_o u_o(\omega_v c_{p,v} + \omega_a c_{p,a}) \quad (13)$$

$$k_{eff} = (1-\varphi)k_s + \varphi\{S_w k_w + S_o k_o + S_g(\omega_v k_v + \omega_a k_a)\} \quad (14)$$

2.3 Boundary and Initial Conditions

The boundary conditions for all variables are:

B.C. for eq. (8): $P_{surf} = P_{fryer}$

B.C. for eq. (10): $q_{surf} = h(T_{oil} - T) - (\lambda + c_{p,w}T)n_{w,surf} - c_{p,v}Tn_{v,surf} - c_{p,o}T_{oil}n_{o,surf}$

B.C. for eq. (1): $n_{w,surf} = u_w\rho_w + h_m\varphi S_w(\rho_{g,surf}\omega_{v,surf} - \rho_{v,fryer})$

B.C. for eq. (6): $n_{v,surf} = u_g\rho_g\omega_v + h_m\varphi S_g(\rho_{g,surf}\omega_{v,surf} - \rho_{v,fryer})$

B.C. for eq. (2): $S_{o,surf} = \text{Table 1}$

B.C. for eq. (3): $n_{AA,surf} = 0$

During frying, the potatoes are assumed to have a constant residual oil on the boundary, and as such, have a certain surface saturation value. This is in agreement with the model of Halder et al. (2007) and Moreira et al. (1997). The saturation value was iterated for to obtain a final oil content close to experimental data.

The initial conditions at *t = 0* are zero for oil saturation, zero for acrylamide concentration, and 298 K for temperature. The initial water saturation is assumed to be 0.8 and the water vapor fraction is calculated from the equilibrium vapor fraction.

2.4 Input parameters

The specific heat capacity of liquid water, water-vapor, and air are temperature dependent, as is the thermal conductivity of water (Halder et al., 2007).

$$c_{p,w} = 4176.2 - 0.0909(T-273) + 5.4731\times10^{-3}(T-273)^2 \quad (15)$$

$$c_{p,v} = 1790 + 0.107(T-273) + 5.856\times10^{-4}(T-273)^2 - 1.997\times10^{-7}(T-273)^3 \quad (16)$$

$$c_{p,a} = 1004.828 - 0.01185(T-273) + 4.300\times10^{-4}(T-273)^2 \quad (17)$$

$$k_w = 0.57109 + 1.762\times10^{-3}(T-273) - 6.7036\times10^{-6}(T-273)^2 \quad (18)$$

The thermal conductivity of oil, water vapor, air, and solid are 0.17, 0.026, 0.026, and 0.21 W m^{-1} K^{-1} respectively and the specific heat of oil and solid are 2223 and 1650 J kg^{-1} K^{-1} respectively.

Relative permeability depends on the amount of liquid water in the system (Bear, 1972). Without loss of generality, the relative permeability of gas was changed for numerical reasons.

$$k_{r,g}^p = S_g \quad (19)$$

$$k_{r,w}^p = \begin{cases} \left(\frac{S_w - 0.08}{1-0.08}\right)^3 & S_w > 0.08 \\ 0 & S_w \le 0.08 \end{cases} \quad (20)$$

$$k_{r,o}^p = \begin{cases} \left(\frac{S_o - 0.08}{1-0.08}\right)^3 & S_o > 0.08 \\ 0 & S_o \le 0.08 \end{cases} \quad (21)$$

Intrinsic permeability is a property of the material and not the fluid. Therefore, intrinsic permeability measurements should be independent of weather a gas or liquid is used. On the contrary, it has been shown that there is a dependence of the gas intrinsic permeability on the pore pressure known as the Klinkenberg effect. The Klinkenberg effect is when gases experience "slip flow" due to the pore radius approaching the mean free path of the particle (Tanikawa and Shimamoto, 2009). In porous media with „low" intrinsic permeability or low pore pressures, the gas intrinsic permeability is expected to be much greater than that of the liquid. The intrinsic permeability of gas used in this model was modified from Halder et al. (2007) to include the correction given by Tanikawa and Shimamoto (2009).

$$k_{in,g}^p = k_{in,w}^p\left(1 + \frac{0.15 k_{in,w}^{p\ -0.37}}{p}\right) \quad (22)$$

For this work, an intrinsic liquid permeability of 1×10^{-15} m^2 was used.

For computational purposes, the density of water $\rho_w = 1036 - 0.1276T - 0.0029(T-273)^2$ and

the potato $\rho_s = 1550 - 0.3(T - 273)$ were assumed to be constant at the arithmetic average of the initial and oil temperatures. The density of gas comes from the ideal gas equation while density of the oil is 879 kg m^{-3}.

As temperature increases, the viscosity changes significantly affecting the velocity of the given species. The viscosity of water (McCabe et al., 2005) $\mu_w = 2.74\times10^{-6}\exp(1735.5/T)$, oil (Halder et al., 2007) $\mu_o = 5.05\times10^{-6}\exp(2725/T)$, and air (McCabe et al., 2005) $\mu_g = 0.017\times10^{-3}(T/273)^{0.65}$ were modeled as a function of temperature. The viscosity of gases is nearly independent of pressure within the ideal gas region.

The Chilton-Colburn analogy (Incropera and DeWitt, 1990) was used to calculate the convective mass transfer coefficient, h_m. The Chilton-Colburn analogy was modified because freezing occurred during vacuum frying simulations with the original expression.

$$h_m = 0.25\frac{hD_{eff,g}\left(\frac{k_v}{\rho_g c_{p,g} D_{eff,g}}\right)^{1/3}}{k_v} \quad (23)$$

The convective heat transfer coefficient is unavailable and difficult to measure for atmospheric and vacuum frying of potato chips. It is not something easily obtained for a thin material since the surface temperature needs to be measured. Its variation with time, such as described by Hubbard and Farkas (1999), is likely different due to the operating conditions and chip size. Yagua and Moreira (2011) used the method of Hubbard and Farkas (1999) to calculate *h* from experimental data for vacuum frying. They found similar profiles to Hubbard and Farkas (1999) but with a maximum *h* value of approximately 2400 W/m^2K. The one problem with this method in determining the value is that is assumes all transferred heat goes into vaporizing water which is then convected away. When in reality, a high portion of the liquid water is convected away before ever being vaporized therefore leading to a much lower value. This phenomenon is more pronounced in products with a small (~1 mm) characteristic length.

For the following model, *h* was estimated to give a reasonable fit to the experimental moisture data. The values used are presented in Table 1 and are similar to the values used by Sahin et al. (1999).

Table 1. Convective heat transfer coefficient and oil saturation boundary condition

Fryer pressure (kPa)	T_{oil} (°C)	Convective heat transfer coefficient, W m^{-2} K^{-1}	Oil saturation at the boundary
101	**150**	85	0.145
	165	90	0.147
	180	85	0.141
16.7	**118**	65	0.086
	132	70	0.09
	144	70	0.097
9.89	**118**	70	0.09
	132	72	0.104
	144	70	0.103
1.33	**118**	60	0.107
	125	70	0.097
	140	90	0.116

3. Numerical Implementation in COMSOL

COMSOL 3.5a was used with the UMFPACK solver. A mapped quadrilateral with a linear distribution was used on the geometry in Figure 1. The left and right boundaries had 75 elements while the top and bottom had 3 elements. A time step of 0.01 was used. The relative and absolute tolerances were set to 10^{-4} and 10^{-6} respectively. The "Convection and Diffusion" module was used to solve for water, oil, and acrylamide mass conservation while "Maxwell-Stefan Diffusion and Convection" was used to gas mass fraction except when the fryer pressure was 1.33 kPa. The mass fraction of water vapor was assumed to be one at 1.33 kPa. "Darcy's Law" and "Convection and Conduction" were used to solve for pressure and temperature respectively.

4. Results and Discussion

4.1 Temperature Distribution

Figure 2 shows the spatial temperature rapidly increases and plateaus as in experimental results (Vitrac et al., 2000) for thin chips (1.5 mm thickness). During the plateau region, there are dips due to evaporation as in the

aforementioned experiments caused by spatial shifts of liquid water causing cooling. Followed by the rapid heating and plateau, the temperature rapidly rises from a lower water content, until asymptotically approaching the oil temperature.

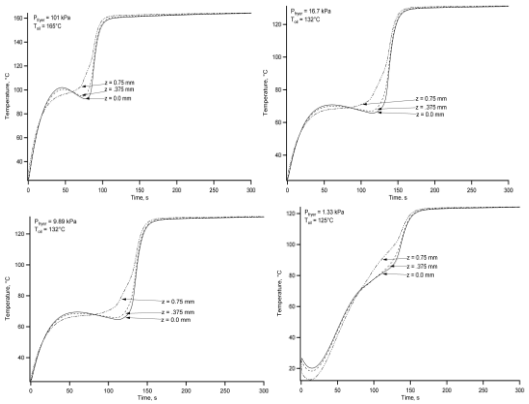

Figure 2. Spatial temperature profiles for: (top left) T_{oil}=165ºC and P_{fryer}=101 kPa, (top right) T_{oil}=132ºC and P_{fryer}=16.7 kPa, (bottom left) T_{oil}=132ºC and P_{fryer}=9.89 kPa, and (bottom right) T_{oil}=125ºC and P_{fryer}=1.33 kPa

In the case of atmospheric and vacuum frying, the temperature does not plateau at the expected boiling point that corresponds to the fryer pressure (11.2°C at 1.33 kPa; 45.6°C at 9.89 kPa; 56.2°C at 16.7 kPa, 100°C at 101 kPa) but rather at a temperature based on the core pressure, intrinsic permeability, and convective mass transfer coefficient. A lower intrinsic permeability causes a higher vapor pressure and therefore a higher boiling temperature. A lower convective mass transfer coefficient forces gas to stay within the chip longer, causing less cooling from less evaporation. The temperature does not plateau for simulations at 1.33 kPa because of the high convective mass transfer coefficient which reduces the amount of trapped gas. The core temperature and pressure for a lower convective mass transfer coefficient are in Figure 3. The results in Figure 2 qualitatively agree with Yagua and Moreira (2011) which show the internal temperature is affected by the fryer pressure and the pressure within the chip.

Figure 3 shows the pressure gradient from the core to the ambient which agrees in magnitude with other experimental results for a starch and alginate experiment (Vitrac et al., 2000). They found a maximum difference of 45 kPa and 10 kPa for alginate without starch and alginate with starch, respectively.

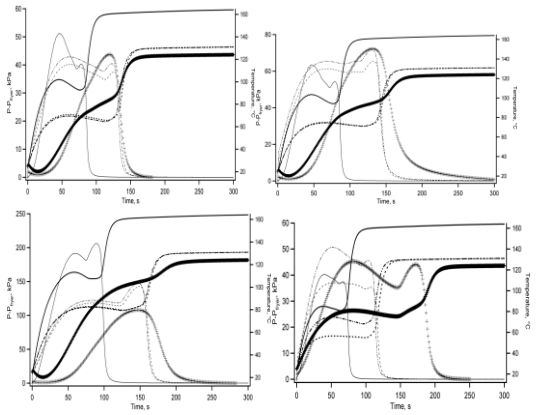

Figure 3. Difference between core pressure and fryer pressure and core temperatures versus time for (top left) model, as is, (top right) no Klinkenberg effect, (bottom left) $k^{P}_{in,w}$ equal to 10^{-16} m^2, and (bottom right) h_m with a coefficient of 1.0 instead of 0.25 and $D_{eff,g}$ at 101325 for all fryer pressures. In all plots, bold lines are temperature and normal lines are pressure profiles. Solid, dash, dash-dot, and plus signs are T_{oil}=165ºC and P_{fryer}=101 kPa, T_{oil}=132ºC and P_{fryer}=16.7 kPa, T_{oil}=132ºC and P_{fryer}=9.89 kPa, and T_{oil}=125ºC and P_{fryer}=1.33 kPa respectively.

Several authors have found the Chilton-Colburn analogy needed to be adjusted to match experimental results. The contribution of intrinsic permeability and the convective mass transfer coefficient help explain the discrepancy between other simulations and experiments and these results. Figure 3 shows the effects of not correcting for the Klinkenberg effect, the effect of intrinsic permeability, and the effect of the convective mass transfer coefficient on temperature and pressure in the core. The Klinkenberg effect decreased the core pressure and temperature as expected. By not accounting for Knudsen flow, gas was trapped in the chip longer. A lower intrinsic permeability significantly increased the core pressure and temperature. A reduced convective mass transfer coefficient increased the core temperature and pressure. Figure 3 shows that a lower convective gas flux increases the core pressure and the temperature at which it plateaus.

4.2 Moisture loss

Figure 4 shows predicted moisture content that compares well with experimental data (Granda, 2005; Garayo and Moreira, 2002). This approach demonstrates the effectiveness of the non-equilibrium approach for evaporation and a constant convective heat transfer coefficient. It is important to note that experimental moisture content can also have inaccuracies due to evaporation from the chips while exiting the fryer or during pressurization.

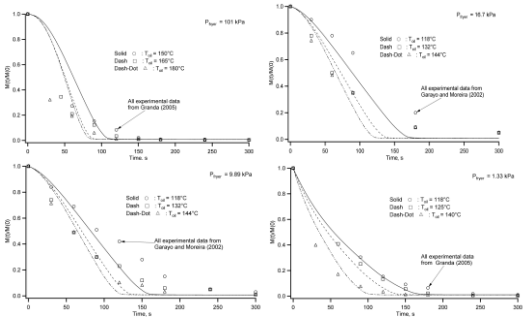

Figure 4. Moisture profile for experimental (dots) and model data (lines) at fryer pressures of: (a) 101 kPa, (b) 16.7 kPa, (c) 9.89 kPa, and (d) 1.33 kPa.

4.3 Oil absorption

Figure 5 shows predicted oil absorption that compares qualitatively with experimental data (Granda, 2005; Garayo and Moreira, 2002). The primary discrepancy between predicted and experimental oil content is during the initial stages of frying where there is a lag in oil absorption in experimental data. The lack of a lag in the predicted oil content is likely due to the convective (outward) flux from the pressure gradient being much less in magnitude than the diffusive (inward) flux of oil. The formulation of oil diffusivity could possibly explain this discrepancy. The oil permeability and diffusivity in the model are unable to capture the effect of changing pore size and other physical changes in the potato chip during crust formation. Collapsing and expanding pores, along with gelatinization of the potato starch greatly affects permeability. Figure 3 possibly confirms the hypothesis that the diffusivity needs reformulating and not the convective flux by showing a high pressure gradient between the core and surface which should lead to a high convective (outward) flux of oil and hence a lag in predicted oil absorption. This hypothesis is similar to that of Vitrac et al. (2000).

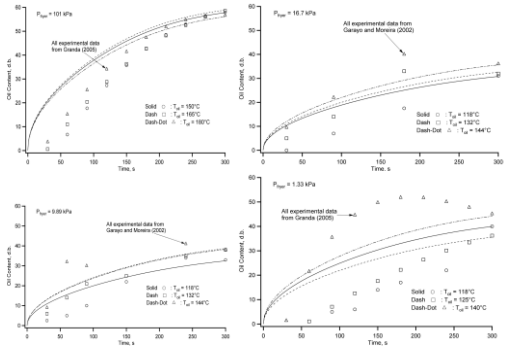

Figure 5. Oil content during frying for experimental (dots) and model data (lines) at fryer pressures of: (top left) 101 kPa, (top right) 16.7 kPa, (bottom left) 9.89 kPa, and (bottom right) 1.33 kPa.

Table 1 shows a general trend towards a lower boundary oil saturation as the fryer pressure is lowered. A hypothesis to explain this trend is the Klinkenberg effect. As the pressure is lowered, the gas velocity at the chip surface increases, increasing the resistance for oil penetration at the boundary. From this model, the gas velocity is almost two orders of magnitude greater for vacuum frying at 1.33 kPa than at 101 kPa.

The Klinkenberg can therefore be used to possibly explain discrepancies in experiments with different levels of oil absorption at the surface. A material with lower intrinsic permeability will likely absorb less oil than a material with a higher value. Additionally, as the fryer pressure is decreased to 1% or even 0.1% of an atmosphere, less oil is expected to be absorbed because of the higher gas velocities at the surface. It can therefore be reasoned that if a material is compressed, decreasing intrinsic permeability, and is fried at 1 kPa or lower, significantly less oil should be absorbed due to a high velocity gas creating a temporary boundary between the product and oil.

4.4 Acrylamide Content

Figure 6 shows transient and spatial variations of acrylamide content. Figure 5 shows good comparison between computed acrylamide content and the experimental data of Granda (2005). There is little spatial variation in a product this small. Computations in Figure 6 are based on potato temperatures and the kinetics of acrylamide formation reported by Granda (2005)

who estimated the kinetic parameters using oil temperature. Use of potato temperature instead of oil temperature is an important extension because as chip size increases, the spatial variations can be captured more realistically.

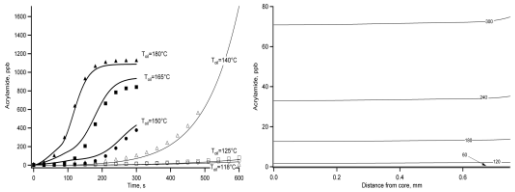

Figure 6. (left) Acrylamide content for experimental fit curve (Granda, 2005) (dots) and model data (lines) where bold is P_{fryer} = 101 kPa and normal is P_{fryer} =1.33 kPa. (right) Local acrylamide content at various times (seconds) for P_{fryer} = 1.33 kPa and T_{oil} = 140ºC

5. Conclusions

Temperature, moisture, pressure, acrylamide content and oil content inside a potato chip during vacuum frying were obtained for the first time using a multiphase porous media transport model. Predictions compared well with experimental data from various researchers. The spatial temperatures increased and plateaued before approaching the oil temperature as in experimental results. Moisture content of simulated and experimental results was comparable while using a non-equilibrium evaporation rate for the simulation. The oil content was qualitatively similar to experimental results. Regardless of the frying pressure, the core experienced pressures of approximately 40 kPa higher than the surface. The Klinkenberg effect was added to the previously developed transport model to account for lower pressures and the potato‟s low intrinsic permeability. Acrylamide concentration matched experimental results with the use of potato temperature instead of oil temperature. This is an important extension because as chip size increases, the spatial variations can be realistically captured.

6. References

1. Bear, J., *Dynamics of Fluids in Porous Media,* American Elsevier Publishing Company, New York (1972)

2. Da Silva, P.F. and Moreira, R.G., Vacuum frying of high-quality fruit and vegetable-based snacks. *Lwt-Food Science and Technology* 41(10), 1758-1767 (2008)

3. Granda, C., Kinetics of acrylamide formation in potato chips. Masters of Science Thesis (Texas A&M University, USA) (2005)

4. Garayo, J., and Moreira, R., Vacuum frying of potato chips. *Journal of Food Engineering* 55(2), 181-191 (2002).

5. Halder, A., et al., An improved, easily implementable, porous media based model for deep-fat frying - Part I: Model development and input parameters. *Food and Bioproducts Processing* 85(C3), 209-219 (2007)

6. Hubbard, L.J. and Farkas, B.E., A method for determining the convective heat transfer coefficient during immersion frying. *Journal of Food Process Engineering* 22(3), 201-214 (1999)

7. Incropera, F.P. and DeWitt, D.P., Fundamentals of Heat and Mass Transfer. 3rd ed. New York: John Wiley & Sons (1990)

8. McCabe, W., et al., Unit Operations of Chemical Engineering 7thed. McGraw-Hill, Boston (2005).

9. Moreira, R.G., et al., Factors affecting oil uptake in tortilla chips in deep-fat frying. *Journal of Food Engineering* 31(4), 485-498 (1997)

10. Moreira, R, „Frying: Vacuum", Encyclopedia of Agricultural, Food, and Biological Engineering, Second Edition, 1:1, 693-696. (2010)

11. Sahin, S., et al., The determination of convective heat transfer coefficient during frying. *Journal of Food Engineering* 39, 307-311 (1999)

12. Tanikawa, W., Shimamoto, T., Comparison of Klinkenberg-corrected gas permeability and water permeability in sedimentary rocks. *International Journal of Rock Mechanics and Mining Sciences* 46(2), 229-238 (2009).

13. Vitrac, O., et al., Deep-fat frying of food: heat and mass transfer, transformations and reactions inside the frying material. European *Journal of Lipid Science and Technology* 102(8-9), 529-538 (2000)

14. Yagua, C.V., Moreira, R.G. Physical and thermal properties of potato chips during vacuum frying. *Journal of Food Engineering* 104(2), 272-283 (2011)